

## Supplemental material

Figure S1. In vivo HP exposure leads to disassembly of pre-existing PAs.

(A) Correlation between average fluorescence of the same MG1655 *ibpA-yfp* cells before and after HP exposure (300 MPa, 20°C, 15 min) ( $r = 0.9453$ ,  $n = 136$ ,  $p\text{-value} = 8.83 \times 10^{-67}$ ). The bisector is shown as a dashed line for reference. Small differences are likely due to different localizations of the PA-foci relative to the focal plane. (B) Frequency distribution of the number of PAs per MG1655 *ibpA-yfp* cell ( $n = 640$ ) observed after HP exposure (300 MPa, 20°C, 15 min). (C) HP exposure abolishes PA mobility in MG1655 *ibpA-yfp* cells. Representative images of a time-lapse fluorescence microscopy image sequence of the same cells at the indicated times after HP exposure (300 MPa, 20°C, 15 min). YFP epifluorescence images (reporting PAs) in combination with cell outlines are shown. The scale bar corresponds to 1  $\mu\text{m}$ . (D) Fraction of viable cells of the indicated strains before (control) and after HP exposure (300 MPa, 20°C, 15 min), with viability being determined as the ability of a cell ( $n = 300$  per independent experiment) to divide within 3 hours after control or HP exposure. The means of three independent experiments are shown with error bars representing the standard deviation. ND = number of viable cells fell below the detection limit of 0.33 % (dotted black line).

Figure S2. HP disperses PAs similarly in LMM1010 *ibpA-yfp* as in MG1655 *ibpA-yfp* (cfr. Fig. 1).

(A and B) Binned histograms show PA distribution along the relative axial position of the cells as detected in (A) untreated and (B) HP exposed (300 MPa, 20°C, 15 min) LMM1010 *ibpA-yfp* cells. Average number of PA-foci per cell was 1.06 for control cells ( $n = 277$ ) and 4.59 for HP exposed cells ( $n = 232$ ). (C) Correlation between average fluorescence of the same LMM1010 *ibpA-yfp* cells before and after HP exposure (300 MPa, 20°C, 15 min) ( $r = 0.8361$ ,  $n = 36$ ,  $p\text{-value} = 2.97 \times 10^{-10}$ ). The bisector is shown as a dashed line for reference. Small differences are likely due to different localizations of the PA-foci relative to the focal plane. (D) Frequency distribution of the number of PAs per LMM1010 *ibpA-yfp* cell ( $n = 232$ ) observed directly after HP exposure (300 MPa, 20°C, 15 min).

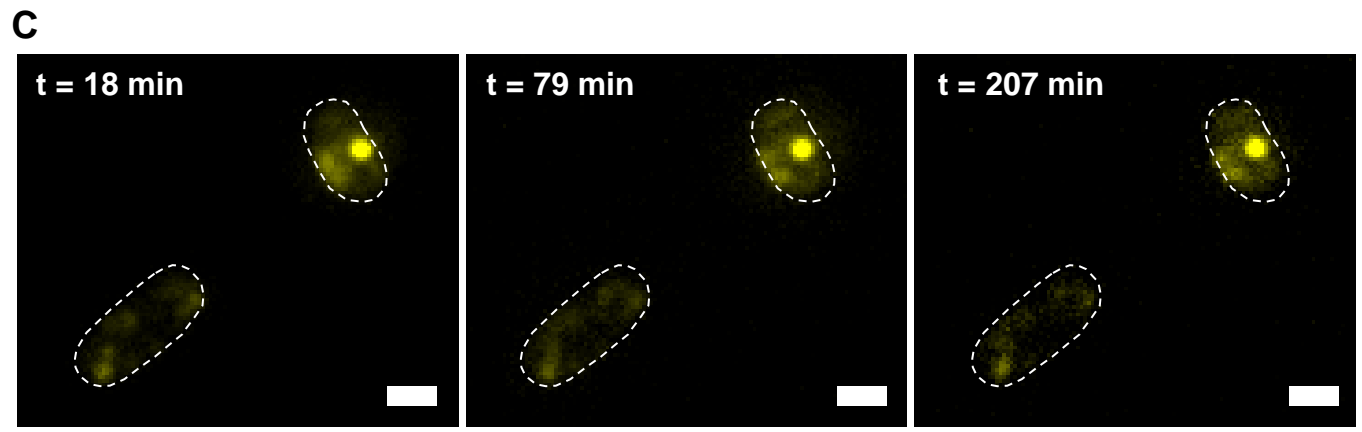
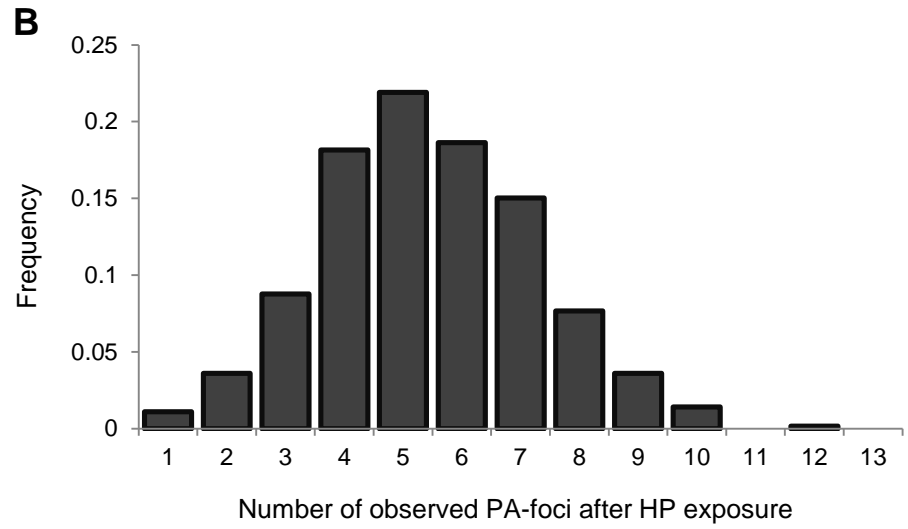
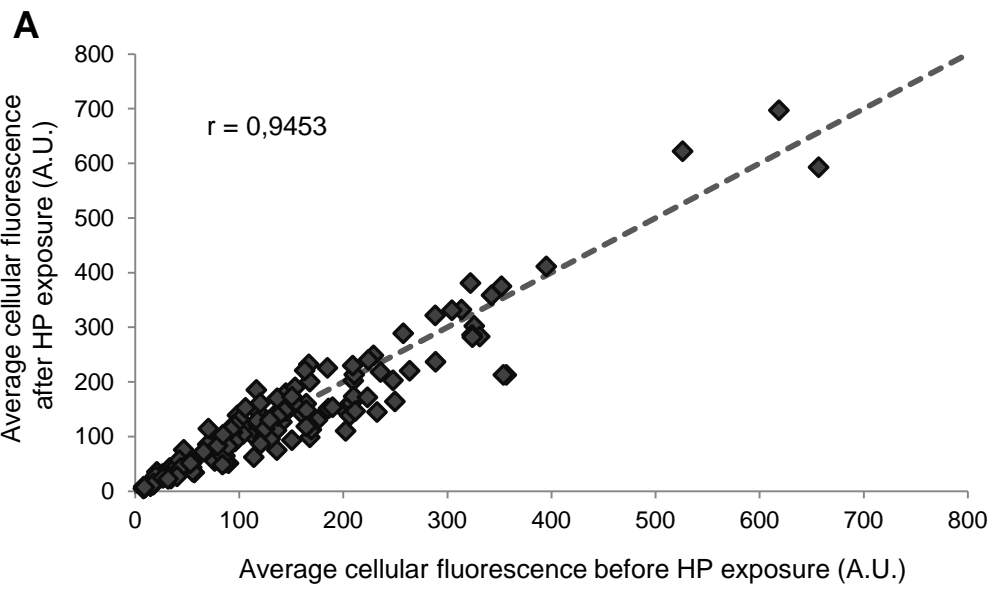
Figure S3. Cellular viability after HP exposure (300 MPa, 20°C, 15 min) is not influenced by CCCP treatment.

Both before and after treatment with the indicated concentration of CCCP survival of cells was determined by spot-plating experiments and expressed as  $\log(N)$ , in which N represents the number of survivors determined by plate counts and expressed as CFU per milliliter.

Figure S4. Polar positioning of PAs is imposed by the nucleoid.

(A and B) Representative images of a time-lapse fluorescence microscopy image sequence of an anucleate LMM1010 *ibpA-yfp ΔrecA* cell (A), and an anucleate MG1655 *ibpA-yfp ΔrecA* cell (B). DAPI (reporting the nucleoid) or YFP (reporting PAs) epifluorescence images in combination with cell outlines are shown at the indicated times after beginning of time lapse recording. The scale bar corresponds to 1  $\mu\text{m}$ .

Figure S1



**D**

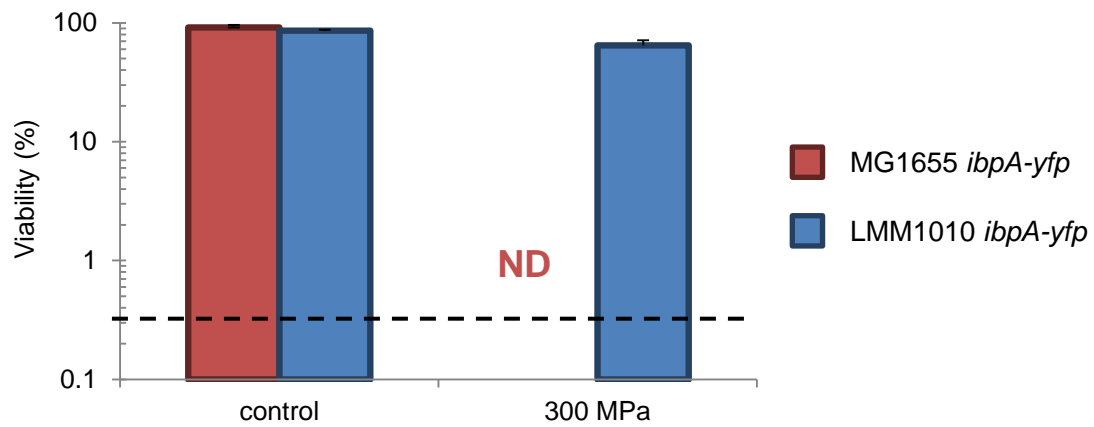


Figure S2

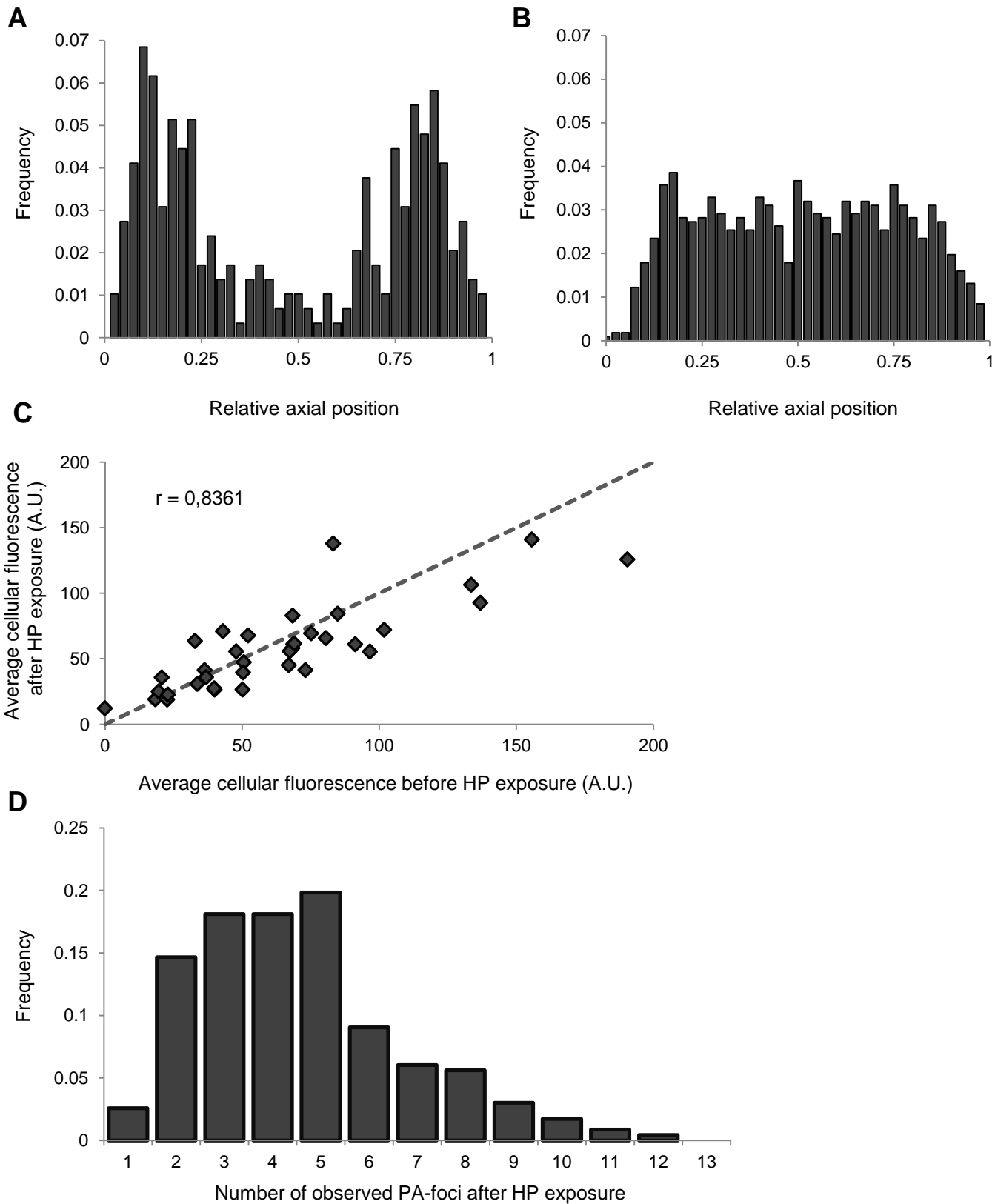


Figure S3

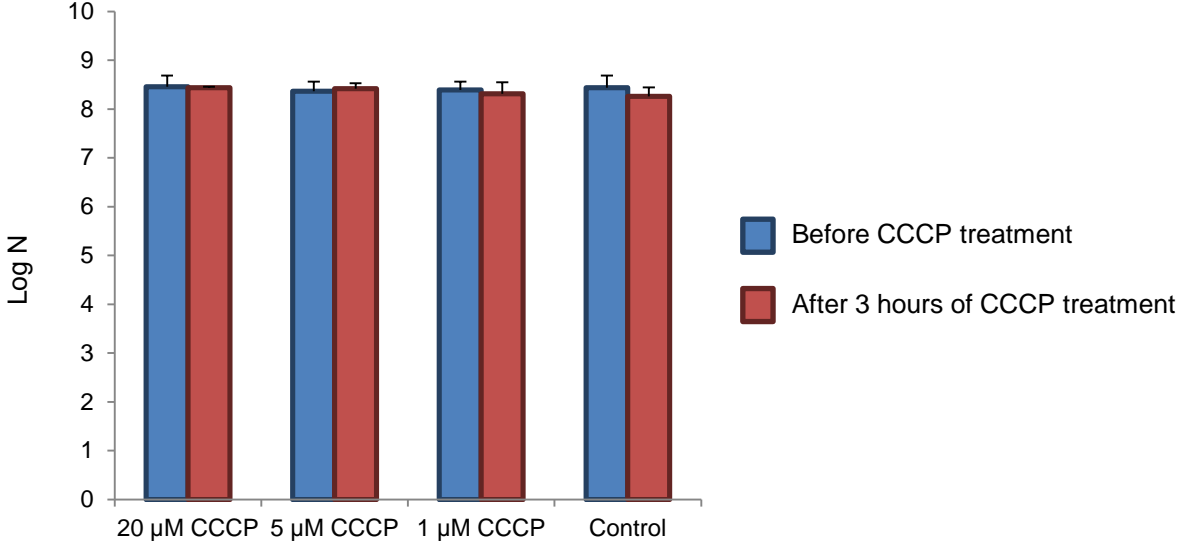
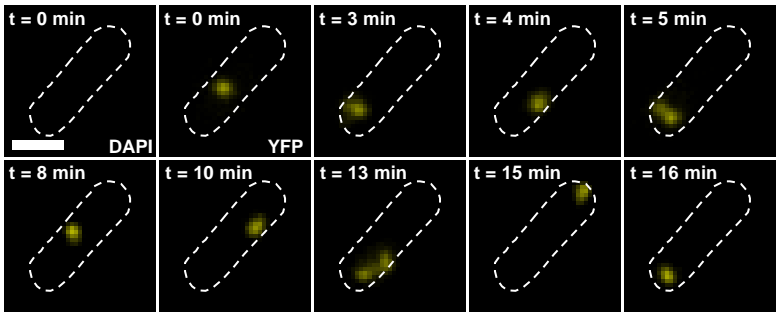


Figure S4

A



B

